Robust colour texture features based on ranklets and discrete Fourier transform

Francesco Bianconi

Università degli Studi di Perugia

Dipartimento Ingegneria Industriale

Via G. Duranti, 67

06125 Perugia (ITALY)

Antonio Fernández, Elena González

Universidade de Vigo

Escuela Técnica Superior de Ingeniería Industrial

Campus Universitario - 36310 Vigo (SPAIN)

Julia Armesto

Universidade de Vigo

Escuela Técnica Superior de Ingeniería de Minas

Campus Universitario - 36310 Vigo (SPAIN)

(Dated: July 8, 2009)

Abstract

In this paper we present a set of multiscale, multidirectional, rotation-invariant features for colour texture characterization. The proposed model is based on the ranklet transform, a technique relying on the calculation of the relative rank of the intensity level of neighbouring pixels. Colour and texture are merged into a compact descriptor by computing the ranklet transform of each colour channel separately and of couples of colour channels jointly. Robustness against rotation is based on the use of circularly symmetric neighbourhoods together with the discrete Fourier transform. Experimental results demonstrate that the approach shows good robustness and accuracy.

I. INTRODUCTION

Texture analysis plays an important role in computer vision. Applications of texture analysis include satellite image segmentation [1], medical diagnosis [2], content-based image retrieval [3], defect detection [4], document processing [5] and surface grading [6–8], to cite some. Within texture analysis, classification is particularly well suited for the automatic grading of products according to the criterion of "same visual appearance". For this reason, an increasing attention from industry has recently emerged, in particular for such products as ceramic tiles [7], marble and granite tiles [9], parquet slabs [10], etc. Since in real applications texture images are rarely acquired under invariable viewing conditions, texture features should be invariant against changes in illumination and viewpoint. Texture analysis has been traditionally performed over gray-scale images. Nowadays, however, it is widely accepted that considering colour can lead to better results [11].

Herein we present a set of robust texture features based on the ranklet transform [12], an image processing technique which considers the relative rank of neighbouring pixels instead of their values. Extension to colour images is obtained by taking account of inter- and intra-channel ranklet features. Self-compensation against rotation is achieved by computing the discrete Fourier transform (DFT) of a set of ranklet features computed from circular neighbourhoods at different rotation angles. The experimental results show that the proposed approach is robust and accurate in discriminating texture.

The remaining of this paper is organized as follows. After a review of related methods (section II), in section III we describe the generalized ranklet transform for colour texture images, and explain how rotation invariance is obtained through DFT compensation of the feature vector. Experimental results are presented in section IV, followed by conclusions (section V).

II. RELATED RESEARCH

Texture analysis has been traditionally performed by extracting texture features from the gray levels of the images, and thus discarding colour information. Many approaches to gray-scale texture analysis have been proposed in the last three decades. For a comprehensive review readers are referred to references [13–16]. Recent experimental work put in evidence

2

that incorporating colour information into the texture model yields improved performance [11]. For this reason there has been a growing interest during the last years in extending traditional gray-scale texture analysis to colour images. Despite many methods for colour texture analysis have been presented in the last years, there is no general framework to classify the wide variety of them. Some attempts to provide a general scheme to organize the various colour texture analysis methods have been published in the past [17, 18]. Unfortunately they are getting out of date, and thus do not embrace some of the most recent approaches. Herein we propose to classify the texture descriptors into three main categories: *spatial*, *spectral* and *hybrid*.

Spatial methods take into account the relative variation of pixel values in the spatial domain. Such kind of analysis can be carried out by considering one or more chromatic channels, and thus the spatial methods can be further subdivided into: *single-channel* and *multiple-channel*. Single-channel techniques are often obtained by straightforward application of gray-scale techniques to colour images which are previously converted into single-channel through colour indexing: the colour histogram undergoes a clustering procedure which returns a set of most representative colours, and the original colours are replaced by their indices. The index pattern is then processed as a gray-scale texture. Such methods are also referred to as *sequential approaches* [17]. In this context it is worth mentioning the extension of the co-occurrence matrix to indexed images [19–21]. Multiple-channel methods consider the spatial structure either within each individual channel or between pairs of channels. Many of these methods have been obtained as extensions of classical gray-scale texture descriptors, such as wavelets [22], Gabor filters [23], co-occurrence matrices [17], Local Binary Patterns [24] and Markov Random Fields [25].

Spectral methods rely solely on the spectral content of the image irrespective of the spatial distribution and, therefore, they are invariant to any permutation of the position of the pixels in the input image. Although there are some methods based on the analysis of the actual spectra [26, 27], most commonly the approaches belonging to this group are focused on the colour content of the image. Such methods aim at giving a statistical description of the colour content of an image. To this purpose one can use global statistical parameters (such as mean value, standard deviation, median, percentiles, etc.) computed directly from the colour data [7, 26, 28]. Such parameters are usually referred to as *soft colour texture descriptors* [7]. Alternatively the colour content can be described by estimating its probability distribution.

This can be done through full multidimensional histograms, such as the colour histogram of Swain and Ballard [29], or by considering the colour distribution in each channel ignoring information about the other channels (marginal histograms) [30, 31]. Other approaches have also been proposed, such as the one of Paschos [32] which is based on computing moments from the probability distribution in the chromaticity diagram.

Hybrid methods share properties of both spatial and spectral methods, although they cannot be considered pure spatial nor pure spectral. There is a wide variety of ways to combine spatial and spectral features into an hybrid model. Such methods include concatenation of textural and colour features [11, 33], fusion of classifiers [34, 35] and joint distribution of colour and texture features [36].

Since ranklets are a relatively recent method, the number of papers related to this concept is rather limited, if compared with other well established methods such as Gabor filters, wavelets, etc. Nonetheless the interest in ranklet-based methods has constantly increased during the last few years. Originally introduced by Smeraldi, who proposed the use of ranklets in face detection [12, 37], the technique has been later applied to computer-aided classification of mammograms [38–40]. Recently Masotti and Campanini [41] proved the effectiveness of ranklets in gray-scale texture classification.

In the next section we introduce the basic concepts about ranklets and then describe our multidirectional and rotation-invariant extension for colour texture characterization.

III. DESCRIPTION OF THE METHOD

The *rank transform* is a non-parametric local measure of relative intensity: it is defined as the number of pixels in a region whose intensity is less than the intensity of the central pixel [42]. Since the rank transform relies on pairwise comparison of pixel values, it is by definition invariant to any monotonic change in the intensity of the input image. Another important property is robustness against noise [43]. The rank transform is the basis of a family of multiscale, orientation-selective, non-parametric features, called *ranklets*, to emphasize their close analogy to Haar wavelets [44]. In previous papers ranklets were defined for gray-scale images by splitting a variable-sized square cluster of pixels into two subsets with the same cardinality, this pair of subsets being defined differently for the horizontal, vertical and diagonal directions, which were the only ones considered (Fig. 1). Orientation-selective

analysis was then attained by measuring the relative frequency with which a pixel in one subset has a gray-scale level higher than a pixel in the other subset, and rotation invariance by averaging the features resulting from the three configurations of Fig. 1. In order to achieve rotation invariant ranklet-based features for colour texture, we extended the idea above in several aspects, which are described in the following subsections.

A. Circular symmetry

It should be noticed that analyzing the subsets of a square cluster of pixels at three orientations only may result in insufficient texture discrimination capability. To overcome this limitation, we both increased the number of orientations and used circularly symmetric clusters, in a similar way to that adopted for Local Binary Patterns [45].

Let's consider an image of $X \times Y$ pixels, and a square window of $n \times n$ pixels, being n an even number. When the image is sequentially scanned with this square window in one-pixel steps, the number of different positions is $Q = (X - n + 1) \times (Y - n + 1)$. Since n is even, the successive positions of the center of the cluster and the image pixels do not overlap. In order to have circular symmetry, we transform the original square window into a circular lattice (Fig. 2) with the same cardinality (n^2). The intensity values of the circular lattice locations which do not fall exactly in the centre of pixels, are estimated through bilinear interpolation. In figure 2 it is shown how a 4×4 square window is converted into the corresponding circular lattice. In this case the locations of the circular lattice lie on concentric circumferences, the diameters of which are d and $2d$ respectively, being d the pixel size.

Now let $C_n(q)$ denote the set formed by the radial lattice locations when the scanning window is in the q-th position, $1 \leqslant q \leqslant Q$. The circular lattice can be split into two subsets in different ways. Following an approach similar to the one proposed for the original ranklets [12, 41] we considered the subsets that can be generated by a single split line (fig. 2, left) and by two orthogonal split lines (fig. 2, right). The orientation of these subsets is defined by the angle θ formed with the horizontal direction. This way the circular lattice is split into two disjoint orientation-dependent subsets $A_{n,m}(q)$ and $B_{n,m}(q)$, where the dependence on size (n), orientation (m) and position (q) has been explicitly specified (Fig. 2). In our implementation we assume that θ is an integer multiple of a given angle $\Delta = \pi/M$, being M is the total number of orientations considered. This means that $\theta = m\Delta$, with
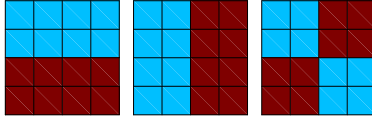
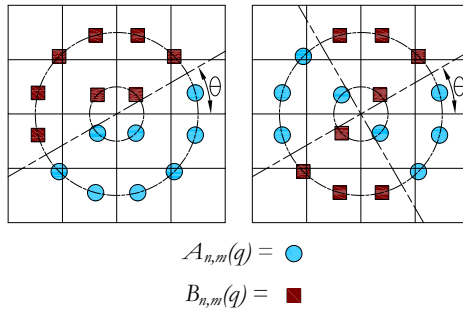FIG. 1: The partitions of a 4×4 cluster into two subsets used in the original gray-scale ranklets.

$A_{n,m}(q) = $ ◯
$B_{n,m}(q) = $ ■

FIG. 2: The partitions of a 4×4 cluster into two subsets used in the generalized ranklets.

$m \in \{0, 1, \ldots, (M-1)\}$.

B. Generalized ranklets

Digital colour images are usually composed of three colour channels, each one containing the values of the colour coordinates in a given colour space (RGB, HSV, CIE L*a*b*, etc.). Our generalization of the ranklet transform to colour textures consists in applying the basic ranklet transform both within and between colour channels in the RGB space. The use of inter-channel features stems from the opponent process theory of the human color vision. This model has been first implemented in a colour texture descriptor by Jain and Healey [23]. Later on the same idea was further developed by Mäenpää and Pietikäinen in the Opponent Colour LBP [46], and by Arvis et al. [19] for the extension of the co-occurrence matrix to colour images. The rationale behind this method is to mimic the human vision system, which perceives colours as two opposing pairs: red/green and yellow/blue. In computer vision this model is generalized by taking into account the three opposing pairs red/green, red/blue and green/blue [46]. The experimental results (sec. IV) validate the effectiveness of this model.

Let $I_i(l)$ and $I_j(l)$ denote the intensity levels corresponding to the i-th and j-th channels,

at a lattice location l, with $i, j \in \{1, 2, 3\}$. If we now consider a circular lattice of n^2 points and a given angle $\theta = m\Delta$, the *generalized rank transform* for scale n and orientation $m\Delta$ between the i and j channels at the position q is defined as:

$$\Re_{n,m}^{i,j}(q) = \frac{1}{n^2/4} \left| \sum_{a \in A_{n,m}(q)} \sum_{b \in B_{n,m}(q)} \xi[I_i(a), I_j(b)] \right| \tag{1}$$

where a and b represent a generic point of the aforementioned subsets $A_{n,m}(q)$ and $B_{n,m}(q)$, and the function $\xi(x, y)$ is defined as follows:

$$\xi(x, y) = \begin{cases} -1 & : & x < y \\ 0 & : & x = y \\ 1 & : & x > y \end{cases} \tag{2}$$

We can see that $(n/2)^2$ pairs of intensities have to be compared at each window position. The computational complexity can be reduced from $O(N^2)$ to $O(NlogN)$ by considering the relative rank of pixels instead of comparing their intensity values [41]. The multiplicative factor in Eq. 1 normalizes the value of the ranklet to $[0, 1]$. Values close to one are related to significant gray-scale variation between the two subsets of pixels, whereas values close to zero indicate no significant difference. It turns out immediately that the generalized ranklet transform as a function of θ is periodic with period π when the subsets are generated by one split line, and with period $\pi/2$ when the subsets are generated by two orthogonal split lines.

The generalized ranklets have a straightforward geometric interpretation: in the case of subsets defined by one splitting line they respond to the presence of edges along the direction θ; in the case of subsets defined by two orthogonal splitting lines they are sensitive to corners formed by two orthogonal lines, one of them forming and angle θ with the horizontal direction. The generalized ranklet transform performs colour texture analysis in two different ways: when $i = j$, ranklets encompass the structural information of a single channel, as gray-scale ranklets do; when $i \neq j$, they reflect the joint structural information between two channels.

C. Feature extraction

Once the generalized ranklets have been computed, the texture features are extracted from each ranklet transform by taking the mean and the standard deviation of the ranklet values:

$$\mu_{n,m}^{i,j} = \frac{1}{Q} \sum_{q=1}^{Q} \Re_{n,m}^{i,j}(q) \tag{3}$$

$$\sigma_{n,m}^{i,j} = \frac{1}{Q-1} \sum_{q=1}^{Q} \sqrt{(\Re_{n,m}^{i,j}(q) - \mu_{n,m}^{i,j})^2} \tag{4}$$

where q denotes a particular position of the center of the cluster during the scanning. The use of the mean and standard deviation is a common practice in feature extraction. These statistics are extensively adopted in texture descriptors such as Gabor filters and wavelets, since they provide, in a compact form, adequate information about the underlying statistical distribution of the texture features throughout the image. The resulting feature set obtained for N different window sizes and M different orientations provides multiscale and orientation-selective texture description.

The above introduced feature set represents an efficient colour texture descriptor. This texture model, however, is still sensitive to rotation. Let's consider the effect of rotation over these features. Let $\mathbf{x} = [x_0, x_1, \ldots, x_{M-1}]$ the vector formed by the M ranklet-based features (mean values or standard deviations) obtained for a given pair of colour channels (i,j) and a given window size n. For the sake of simplicity, but without loss of generality, we dropped the i, j and n dependence from the above expression. As a result of the features definition, if we rotate a texture by an angle Δ and compute the same ranklet-based features over the rotated texture, the resulting vector $\mathbf{x}'$ will be circularly-shifted by one position: $\mathbf{x}' = [x_1, \ldots, x_{M-1}, x_0]$.

As a consequence, sensitivity against rotation can be removed by taking the discrete Fourier transform of the feature vector $\mathbf{x}$. If $\mathbf{X} = [X_0, X_1, \ldots, X_{M-1}]$ is the DFT of vector $\mathbf{x}$, a circular shift to $\mathbf{x}$ corresponds to multiplying the complex coefficients X_k by a linear phase factor. Hence, the modulus of the transformed coefficients $|X_k|$ is independent of any circular shift of the input vector $\mathbf{x}$. In addition we know that the DFT output is half redundant, and therefore we get the complete information by looking at the first $[(M/2)+1]$

elements of the transformed vector [47], where [·] denotes "integer part of".

Thus the rotation-invariant feature vector representative of a colour texture is as follows:

$$\mathbf{r} = \left[\mathbf{\Phi}_1^{i,j}, \cdots, \mathbf{\Phi}_N^{i,j}, \mathbf{\Psi}_1^{i,j}, \cdots, \mathbf{\Psi}_N^{i,j} \right] \qquad (5)$$

where $\mathbf{\Phi}_n^{i,j}$ and $\mathbf{\Psi}_n^{i,j}$ are the vectors formed by the modulus of the first $[(M/2)+1]$ terms of the DFT of $\boldsymbol{\mu}_n^{i,j} = [\mu_{n,0}^{i,j}, \mu_{n,1}^{i,j}, \ldots, \mu_{n,M-1}^{i,j}]$ and $\boldsymbol{\sigma}_n^{i,j} = [\sigma_{n,0}^{i,j}, \sigma_{n,1}^{i,j}, \ldots, \sigma_{n,M-1}^{i,j}]$ respectively.

For a 3-channel image, we have six possible channel combinations, namely $(i,j) \in \{(1,1),(2,2),(3,3),(1,2),(1,3),(2,3)\}$, the first three ones corresponding to the intra-channel case, and the remaining to the inter-channel case. If we perform multiscale analysis for N different values of n, and orientation-selective analysis for M_1 different angles of subsets defined by one split line and M_2 different angles of subsets defined by two split lines, the resulting dimension of the feature space is given by:

$$p = 2 \times 6 \times N \times \left([\frac{M_1}{2} + 1] + [\frac{M_2}{2} + 1] \right) \qquad (6)$$
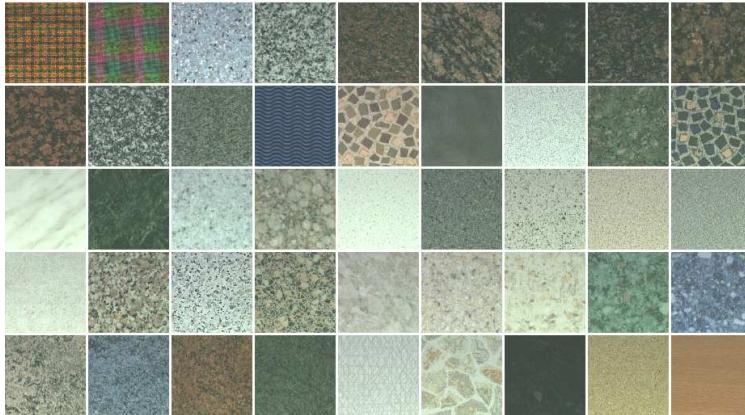
IV. EXPERIMENTAL RESULTS

FIG. 3: The 45 colour texture images used in the experiments.

To assess the performance of the proposed feature set, we carried out a texture classification experiment. Our benchmark data consists of 45 colour textures from the Outex library (fig. 3). The textures used here are a subset of the group *inca 100dpi*. The database is composed of hardware-rotated versions of the 45 texture images taken at 9 different

orientations, namely $0°, 5°, 10°, 15°, 30°, 45°, 60°, 75°$ and $90°$ (which are the only available orientations in the OuTex database).

As a first step the original RGB images have been converted into the sRGB colour space. This colour space possesses two desirable features: 1) it is device independent, and 2) it has been adopted as the default colour space for the internet [48]. The use of a device-independent colour space eliminates the bias which affects device-dependent data. In order to convert the original RGB data to the sRGB space we developed a colour calibration procedure which takes as input the spectral sensitivity of the camera and the spectra of the illuminant used for image acquisition (data available at http://www.outex.oulu.fi). For a detailed description of the method readers are referred to reference [49].

After the colour conversion step, each texture image was subdivided into 16 non-overlapping sub-images, resulting in a database of $45 \times 16 \times 9 = 6480$ texture samples, 720 for each rotation angle. In order to assess robustness against rotation, we conducted a separate classification trial for each rotation angle in the following way:

- We randomly split the 16 samples of each texture class into two groups of 8 texture samples each: one for training and the other one for testing. The 8 texture samples used for training are always picked from the $0°$ group, while the 8 texture samples for testing are picked from the α-degree group, where $\alpha = \{0°, 5°, 10°, 15°, 30°, 45°, 60°, 75°, 90°\}$. For each angle this results in a training set of $45 \times 8 = 360$ non rotated texture samples, and a test set of $45 \times 8 = 360$ rotated texture samples. This procedure is usually referred to as *split-half validation* [50].

- The samples of the test set are classified according to the nearest neighbour rule with the "Manhattan" (L1) distance, and the percentage of correct classification is evaluated.

- In order to obtain a stable error estimation the random subdivision into train set and test set is repeated 100 times, and the average classification accuracy over the 100 problems is retained.

Table I resumes the results of our approach. In order to separately validate the effects of the inclusion of inter-channel features compared to intra-channel features, we implemented three versions of the generalized ranklets: a single-channel version (used with gray-scale

images), a version with intra-channel features only and a version with intra-channel and inter-channel features. Moreover, in order to validate the rotation-invariance introduced through the DFT, we reported the results obtained both with and without DFT normalization. In all cases the texture features are based on generalized ranklets with three resolutions ($n = 4, 6, 8$). For each resolution orientational selectivity is taken into account by considering six subsets generated by a single split line $\theta = \{0°, 30°, 60°, 90°, 120°, 150°\}$ (hence $M_1 = 6$ in eq. 6) and three subsets generated by two orthogonal split lines $\theta = \{0°, 30°, 60°\}$ (hence $M_2 = 3$ in eq. 6). Due to the periodic nature of the generalized ranklet transform, it suffices to take $0 \leq \theta < \pi$ in the case of single-line split and $0 \leq \theta < \pi/2$ in the case of double-line split. This results in 54 features for each channel. When DFT is applied the number of features (eq. 6) reduces to 36.

TABLE I: Experimental results. Percentage of correct classification.

Method	DFT	Col. space	Dim.	Mean	Std	0°	5°	10°	15°	30°	45°	60°	75°	90°
Gener. ranklets	NO	GRAY	54	**43,7**	*13,2*	57,9	58,7	57,0	54,6	41,0	34,4	29,8	30,3	29,6
Gener. ranklets	YES	GRAY	36	**58,5**	*2,2*	59,7	61,1	59,6	60,0	60,6	58,2	55,8	55,7	55,9
Gener. ranklets / intra-channel	NO	sRGB	162	**62,3**	*16,5*	79,6	78,8	78,7	77,5	62,5	51,5	45,7	43,8	42,9
Gener. ranklets / intra-channel	YES	sRGB	108	**82,6**	*2,1*	83,7	84,0	84,7	84,4	84,3	82,5	80,8	79,6	79,5
Gener. ranklets / intra- and inter-channel	NO	sRGB	324	**93,2**	*3,7*	96,4	96,6	96,3	96,0	95,1	91,6	90,1	88,7	87,5
Gener. ranklets / intra- and inter-channel	YES	sRGB	216	**96,2**	*0,7*	97,0	96,8	96,7	96,9	96,3	95,5	96,2	95,3	95,1

In order to put our results in the context of related work on the subject, we compared them with the results obtained through a set of ten alternative methods: four pure textural methods, and six joint colour texture descriptors, two for each of the three groups described in section II. The results are summarized in table II.

The pure texture methods cover the original ranklet features presented in [41], and the classical methods of Gabor filters, co-occurrence matrices and Local Binary Patterns (LBP). The original ranklet features are computed using same three resolutions used for the generalized ranklets ($n = 4, 6, 8$). Gabor filters settings are the same used in [51], and rotation invariance is obtained through DFT normalization [47]. Co-occurrence matrices have been implemented adopting the same displacement field and the same features used in [19], and rotation invariance is obtained by summing up the resulting matrices. LBP is used in the rotation-invariant version $\text{LBP}_{8,1}^{ri}$ [45].

TABLE II: Experimental results. Comparison with other methods.

Method	Col. space	Dim.	Mean	Std	0°	5°	10°	15°	30°	45°	60°	75°	90°
Texture only													
Original ranklets	GRAY	18	**54,6**	*2,6*	53,1	54,8	53,0	49,5	58,3	56,5	56,5	54,3	55,2
Gabor filters	GRAY	48	**47,6**	*2,8*	47,5	47,5	47,7	47,8	52,7	45,4	48,9	42,3	49,1
LBP	GRAY	36	**70,9**	*1,1*	70,8	70,5	69,3	70,6	72,4	71,3	71,8	72,0	69,2
Co-occurrence matrices	GRAY	5	**42,2**	*1,5*	42,2	40,7	39,5	42,9	42,8	41,5	44,0	44,1	42,3
Spectral methods													
Colour histogram	sRGB	512	**92,2**	*0,3*	92,1	92,1	91,8	91,9	92,5	92,0	92,7	92,5	92,2
Chromaticity moments	xyY	10	**77,4**	*1,7*	79,1	77,7	78,2	78,5	78,4	78,7	76,4	75,1	74,3
Spatial methods													
Multispectral Gabor filters with opponent col.	sRGB	96	**84,3**	*1,2*	84,0	84,0	84,0	84,3	86,6	83,2	85,3	82,6	84,5
Multispectral co-occurence matrices	sRGB	30	**90,4**	*0,6*	90,1	89,2	90,2	90,7	90,2	91,0	90,8	91,0	90,4
Hybrid methods													
Gabor filters + HLS statistics	GRAY + HLS	52	**77,4**	*1,9*	77,8	77,8	77,8	76,1	80,5	75,6	79,1	74,2	77,9
LBP + RGB Centiles	GRAY + sRGB	51	**94,4**	*0,8*	93,6	93,6	93,6	94,5	94,1	94,3	95,3	95,9	94,2

The spatial group of joint texture and colour methods include two approaches that extend these two methods to colour images. In the case of Gabor filters we adopted the opponent colour approach proposed by Jain and Healey [23] along with DFT normalization to ensure rotation invariance. In the case of co-occurrence matrices we used the multispectral method proposed by Arvis et al. [19].

The spectral methods group encloses the classical colour histogram method of Swain and Ballard [29], and the chromaticity moments proposed by Paschos [32]. The colour histogram was computed using a uniform subdivision of each axis of the colour space in 8 intervals. For the chromaticity moments we used 5 T-type and 5 D-type moments (referred to as the setting "CM55" in [32]).

In the hybrid methods group we considered two approaches were textural features computed from gray-scale images are concatenated with colour features. The first one [33] is based on Gabor features (herein computed again with the same settings used in [51]) and colour statistics extracted from the hue and saturation channels of the HLS colour space. The second one [10] is based on concatenating LBP features (herein we used the rotation invariant version LBP_{81}^{ri} [45]) and colour centiles.

The results reported in tables I and II confirm the positive effect of orientational selec-

tivity in gray-scale texture classification in comparison with the original implementation [41] (mean accuracy 58,5% vs. 54,6%) together with a better rotation invariance (standard deviation 2,2 vs. 2,6). From the experimental results it also emerges the beneficial effect of including intra-channel features compared to single-channel (gray-scale) features (82,6% vs. 58,5%), as well as the advantage of considering both intra- and inter-channel features instead of intra-channel features only (96,2% vs. 82,6%). This finding is in agreement with the results obtained by other authors with different methods [19, 23]. Another important outcome is the positive effect of DFT normalization on invariance against rotation. Comparison with other methods (table II) shows that the generalized ranklets approach is more accurate than the other methods used for comparison. It should be noticed that feature extraction in the proposed method -as in any other rank-based method- is computationally intensive, since sorting of gray levels is a time consuming operation. It is also worth mentioning that the dimension of the feature space is higher than most of the other texture descriptors considered for comparison, which consequently leads to slower classification. In conclusion it turns out that the approach proposed here is computationally demanding but markedly more accurate than the methods considered for comparison. A remarkable exception is the LBP + RGB centiles descriptor, which achieves a lower -yet comparable-accuracy with approximately four times less features.

V. CONCLUSIONS

In this paper we introduced a set of rotation-invariant features based on ranklets for colour texture description. Extension to colour images is obtained by considering inter-channel and intra-channel ranklets. Rotation invariance is based on the use of multidirectional circularly symmetric neighbourhoods whose response is compensated against rotation through the discrete Fourier transform. The experimental results show that this feature set provides very high classification accuracy.

---

[1] X. Hu, V. Tao, and B. Prenzel, "Automatic segmentation of high-resolution satellite imagery by integrating texture, intensity and color features," *Photogrammetric Engineering and Remote Sensing* **71**, 1399–1406 (2005).

[2] B. Acha, C. Serrano, J. Acha, and L. Roa, "Segmentation and classification of burn images by color and texture information," *Journal of Biomedical Optics* **10** (2005).

[3] R. Datta, D. Joshi, J. Li, and J. Wang, "Image retrieval: Ideas, influences, and trends of the new age," *ACM Computing Surveys* **40**, 5:1–5:59 (2008).

[4] K. Song, J. Kittler, and M. Petrou, "Defect detection in random colour texture," *Image Vision and Computing* **14**, 667–683 (1996).

[5] D. Wen and X. Ding, "Visual similarity based document layout analysis," *Journal of Computer Science and Technology* **21**(3), 459–465 (2006).

[6] C. Boukouvalas, J. Kittler, R. Marik, and M. Petrou, "Color grading of randomly textured ceramic tiles using color histograms," *IEEE Transactions on Industrial Electronics* **46**, 219–226 (1999).

[7] F. López, J. Valiente, J. Prats, and A. Ferrer, "Performance evaluation of soft color texture descriptors for surface grading using experimental design and logistic regression," *Pattern Recognition* **41**, 1744–1755 (2008).

[8] F. López, J. Valiente, R. Baldrich, and M. Vanrell, "Fast surface grading using color statistics in the CIE Lab space," *Lecture Notes in Computer Science* **3773**, 13–23 (2005).

[9] F. Bianconi and A. Fernández, "Granite texture classification with Gabor filters," in *Proc. of the 18th International Congress on Graphical Engineering*, (Sitges, Spain) (2006).

[10] M. Niskanen, O. Silvén, and H. Kauppinen, "Color and texture based wood inspection with non-supervised clustering," in *Proceedings of the 12th Scandivanian Conference on Image Analysis*, 336–342, (Bergen, Norway) (2001).

[11] A. Drimbarean and P. Whelan, "Experiments in colour texture analysis," *Pattern Recognition Letters* **22**, 1161–1167 (2001).

[12] F. Smeraldi, "Ranklets: orientation selective non-parametric features applied to face detection," in *Proceedings of the 16th International Conference on Pattern Recognition (ICPR'02)*, **3** (2002).

[13] M. Petrou and P. G. Sevilla, *Image Processing. Dealing with Texture*, Wiley Interscience (2006).

[14] M. Bharati, J. Liu, and J. MacGregor, "Image texture analysis: methods and comparisons," *Chemometrics and intelligent laboratory systems* **72**, 57–71 (2004).

[15] M. Tuceryan and A. Jain, "Texture analysis," in *The Handbook of Pattern Recognition and*

Computer Vision (2nd Edition), C. Chen, L. Pau, and P. Wang, Eds., 207–248, World Scientific Publishing (1998).

[16] X. Xie and M. Mirmehdi, "A galaxy of texture features," in *Handbook of texture analysis*, M. Mirmehdi, X. Xie, and J. Suri, Eds., 375–406, Imperial College Press (2008).

[17] C. Palm, "Color texture classification by integrative co-occurrence matrices," *Pattern Recognition* **37**, 965–976 (2004).

[18] R. Schettini, G. Ciocca, and S. Zuffi, "A survey of methods for colour image indexing and retrieval in image databases," (2001).

[19] V. Arvis, C. Debain, M. Berducat, and A. Benassi, "Generalization of the cooccurrence matrix for colour images: application to colour texture classification," *Image Analysis and Stereology* **23**, 63–72 (2004).

[20] J. Huang, S. Kumar, M. Mitra, W. Zhu, and R. Zabih, "Image indexing using color correlograms," in *Proceedings of the IEEE Conference on Computer Vision and Pattern Recognition*, 762–768, (San Juan, Puerto Rico) (1997).

[21] E. V. den Broek and E. V. Rikxoort, "Evaluation of color representation for texture analysis," in *Proceedings of the 16th Belgium-Netherlands Conference on Artificial Intelligence*, (2004).

[22] G. V. de Wouver, P. Scheunders, S. Livens, and D. V. Dyck, "Wavelet correlation signatures for color texture characterization," *Pattern Recognition* **32**, 443–451 (1999).

[23] A. Jain and G. Healey, "A multiscale representation including opponent color features for texture recognition," *IEEE Transactions on Image Processing* **7**, 124–128 (1998).

[24] M. Pietikäinen, T. Mäenpää, and J. Viertola, "Color texture classification with color histograms and Local Binary Patterns," in *Proceedings 2nd International Workshop on Texture Analysis and Synthesis*, 109–112, (Copenhagen, Denmark) (2002).

[25] D. K. Panjwani and G. Healey, "Markov random field models for unsupervised segmentation of textured color images," *IEEE Transactions on Pattern Analysis and Machine Intelligence* **17**, 939–954 (1995).

[26] S. Kukkonen, H. Kälviäinen, and J. Parkkinen, "Color features for quality control in ceramic tile industry," *Optical Engineering* **40**, 170–177 (2001).

[27] Y. Manabe, K. Sato, and S. Inokuchi, "An object recognition through continuous spectral images," in *Proceedings of the 12th International Conference on Pattern Recognition*, **1**, 858–860.

[28] J. Prats-Montalbán, F. López, J. Valiente, and A. Ferrer, "Multivariate statistical projection methods to perform robust feature extraction and classification in surface grading," *Journal of Electronic Imaging* **17**, 031106–1–10 (2008).

[29] M. Swain and D. Ballard, "Color indexing," *International Journal of Computer Vision* **7**, 11–32 (1991).

[30] M. Pietikäinen, S. Nieminen, E. Marszalec, and T. Ojala, "Accurate color discrimination with classification based on features distributions," in *Proceedings of the 13th International Conference on Pattern Recognition*, **3**, 833–838, (Vienna, Austria) (1996).

[31] L. Lepistö, I. Kunttu, and A. Visa, "Color-based classification of natural rock images using classifier combinations," *Lecture Notes in Computer Science* **3540**, 901–909 (2005).

[32] G. Paschos, "Fast color texture recognition using chromaticity moments," *Pattern Recognition Letters* **21**, 837–841 (2000).

[33] A. Monadjemi, B. Thomas, and M. Mirmedi, "Speed v. accuracy for high resolution colour texture classification," in *Proceedings of the 13th British Machine Vision Conference*, 143–152, (Cardiff, UK) (2002).

[34] E. Kurmyshev and R. Sánchez-Yañez, "Comparative experiment with colour texture classifiers using the CCR feature space," *Pattern Recognition Letters* **26**, 1346–1353 (2005).

[35] L. Lepistö, I. Kunttu, and A. Visa, "Classification of natural rock images using classifier combinations," *Optical Engineering* **45** (2006).

[36] S. Chatzichristofis and Y. Boutalis, "FCTH: Fuzzy color and texture histogram - a low level feature for accurate image retrieval," 191–196 (2008).

[37] F. Smeraldi, "A nonparametric approach to face detection using ranklets," *Lecture Notes in Computer Science* **2688**, 351–359 (2003).

[38] A. Mohamed, R. El-Khoribi, and L. Fekry, "Discrete hidden Markov tree modelling of ranklet transform for mass classification in mammograms," *International Journal on Graphics, Vision and Image Processing* **7**, 61–68 (2007).

[39] W. Kim and S. Kim, "Homogeneity and ranklet based mass-type cancer detection in dense mammographic images," in *Proceedings of the 2nd International Conference on Advanced Nondestructive Evaluation*, S. Lee, J. Lee, I. Park, S. Song, and M. Choi, Eds., 157–162, World Scientific Publishing (2008).

[40] M. Masotti, "A ranklet-based image representation for mass classification in digital mammo-

grams," *Medical Physics* **33**, 3951–3961 (2006).

[41] M. Masotti and R. Campanini, "Texture classification using invariant ranklet features," *Pattern Recognition Letters* **29**, 1980–1986 (2008).

[42] R. Zabih and J. Woodfill, "Non-parametric local transforms for computing visual correspondence," in *Proceedings of the 3rd European Conference on Computer Vision (ECCV)*, 151–158, Springer-Verlag, (Stockholm, Sweden) (1994).

[43] R. M. Hodgson, D. G. Bailey, M. J. Naylor, A. L. Ng, and S. J. McNeill, "Properties, implementations and applications of rank filters," *Image Vision Comput.* **3**(1), 3–14 (1985).

[44] I. Daubechies, *Ten Lectures on Wavelets*, Society for Industrial and Applied Mathematics (1992).

[45] T. Ojala, M. Pietikäinen, and T. Mäenpää, "Multiresolution gray-scale and rotation invariant texture classification with Local Binary Patterns," *IEEE Transactions on Pattern Analysis and Machine Intelligence* **24**, 971–987 (2002).

[46] T. Mäenpää and M. Pietikäinen, "Texture analysis with Local Binary Patterns," in *Handbook of Pattern Recognition and Computer Vision (2nd Edition)*, C. Chen, L. Pau, and P. Wang, Eds., 197–216, World Scientific Publishing (2005).

[47] F. Bianconi, A. Fernández, and A. Mancini, "Assessment of rotation-invariant texture classification through Gabor filters and Discrete Fourier Transform," in *Proc. of the 20th International Congress on Graphical Engineering*, (Valencia, Spain) (2008).

[48] H. Kang, *Computational Color Technology*, Spie Press (2006).

[49] F. Bianconi, A. Fernández, E. González, D. Caride, and A. Calviño, "Rotation-invariant colour texture classification through multilayer CCR," *Pattern Recognition Letters* **30**, 765–773 (2009).

[50] E. Steyerberg, F. Harrell, G. Borsboom, M. Eijkemans, Y. Vergouwe, and J. Habbema, "Internal validation of predictive models: Efficiency of some procedures for logistic regression analysis," *Journal of Clinical Epidemiology* **54**, 774–781 (2001).

[51] B. Manjunath and W. Ma, "Texture features for browsing and retrieval of image data," *IEEE Transactions on Pattern Analysis and Machine Intelligence* **18**, 837–841 (1996).

Francesco Bianconi received a Master degree in Mechanical Engineering in 1997 from the University of Perugia (Italy) and a PhD in Computer-aided Design in 2000 from a consortium of Italian universities. He is currently Assistant Professor of Technical Drawing at the Faculty of Engineering, University of Perugia. He worked as visting researcher at the MIT (USA) and at the University of Vigo (Spain). His research interests cover image processing and CAD/CAE. He is member of ACM and IEEE.

Antonio Fernández was born in Vigo, Spain, in 1967. He graduated as Industrial Engineer (equivalent to MEng) in 1993 and received a PhD in Industrial Engineering (with special distinction) in 1998, both degrees from the University of Vigo, where he developed most of his career. He held a research fellowship in the Department of Applied Physics during the period 1994-1998, and subsequently was an Associate Lecturer with the Department of Engineering Design from 1999 to 2003. Since then he has been a Senior Lecturer, and the Head of the Colorimetry Research Group. He has worked as a visiting researcher at Center for Research on Optics (Mexico), Dublin City University (Ireland), University of Perugia (Italy), and Computer Vision Center (Spain). His major research interests include texture analysis and speckle metrology.

Elena González received a MEng and a PhD in Industrial Engineering in 1985 and 1994, respectively, from the University of Vigo, Spain, where she is currently Senior Lecturer with the Department of Engineering Design. Her research interests cover industrial applications of colour technology and pattern recognition.

Julia Armesto received a MEng and a PhD in Forest Engineering in 2000 and 2004, respectively, from the University of Santiago de Compostela, Spain. She is currently Lecturer with the Department of Natural Resources and Environmental Engineering. Her research interests cover laser scanning, photogrammetric and thermographic technologies, image processing and sensor registration techniques.